A guide to assessing Endoplasmic Reticulum homeostasis and stress in mammalian systems

Daria Sicari, Agnès Delaunay-Moisan, Laurent Combettes, Eric Chevet, Aeid Igbaria

DR ERIC CHEVET (Orcid ID : 0000-0001-5855-4522)

Received Date : 25-Jul-2019
Revised Date : 10-Sep-2019
Accepted Date : 23-Oct-2019

Color : Fig 1
SuppInfo : 1 file

Title: A guide to assessing Endoplasmic Reticulum homeostasis and stress in mammalian systems.

Daria Sicari[1,2], Agnès Delaunay-Moisan[3], Laurent Combettes[4], Eric Chevet[1,2*] and Aeid Igbaria[1,2*]

[1]Inserm U1242, University of Rennes, Rennes, France. [2]Centre de lutte contre le cancer Eugène Marquis, Rennes, France. [3]Institute for Integrative Biology of the Cell (I2BC), CEA-Saclay, CNRS, Université Paris-Saclay, ISVJC/SBIGEM, Laboratoire Stress Oxydant et Cancer, 91191 Gif-sur-Yvette, France. [4]Université Paris Sud, UMRS1174, Orsay F-91405, France; Institut National de la Santé et de la Recherche Médicale (Inserm), UMRS1174, Orsay F-91405, France

*correspondence to EC (eric.chevet@inserm.fr) or AI (aeid.igbaria@gmail.com)

Running Title: tools to measure ER homeostasis in mammals

Keywords: ER stress, UPR, ER redox state, Calcium distribution, ER structure

Abbreviations:

ER stress: Endoplasmic Reticulum stress
ERAD: ER-associated degradation
UPR: Unfolded Protein Response
IRE1: Inositol-requiring protein 1
PERK: PRKR-like endoplasmic reticulum kinase
ATF6: Activating transcription factor 6
XBP1: X-box-binding protein 1
RIDD: RNA IRE1a-dependent decay
Tg: Thapsigargin
Tm: Tunicamycin
DTT: Dithiothreitol
ERSE-I/II: Endoplasmic Reticulum Stress Element I/II
UPRE: UPR Element
sfGFP: superfolder Green Fluorescent Protein
GSH: Glutathione
TXN: Thioredoxin
rxYFP: redox sensitive YFP
roGFP: reduction-oxidation sensitive GFP
FLIM: Intrinsically Lower Fluorescence
AM: Acetomethoxy
GECIs: Genetically Encoded Calcium Indicators
FP: Fluorescent Protein
FRET: Forster resonance energy transfer
EM: Electron Microscopy
ThT: Thioflavin

ABSTRACT

The endoplasmic reticulum (ER) is a multifunctional organelle that constitutes the entry into the secretory pathway. The ER contributes to the maintenance of cellular calcium homeostasis, lipid synthesis and productive secretory and transmembrane protein folding. Physiological, chemical and pathological factors that compromise ER homeostasis lead to ER stress. To cope with this situation, cells activate an adaptive signaling pathway termed the Unfolded Protein Response (UPR) that aims at restoring ER homeostasis. The UPR is transduced through post-translational, translational, post-transcriptional and transcriptional mechanisms initiated by three ER-resident sensors, IRE1□, ATF6□ and PERK. Determining the ins and out of ER homeostasis control and UPR activation still represents a challenge for the community. Hence, standardized criteria and methodologies need to be proposed for monitoring ER homeostasis and ER stress in different model systems. Here, we summarize the pathways that are activated during ER stress and provide approaches aimed at assess ER homeostasis and stress *in vitro* and *in vivo* mammalian systems that can be used by researchers to plan and interpret experiments. We recommend the use of multiple assays to verify ER stress because no individual assay is guaranteed to be the most appropriate one.

INTRODUCTION

The endoplasmic reticulum (ER) represents a complex membranous network that beyond ensuring cell calcium and lipid homeostasis, mediates the productive folding and trafficking of transmembrane and secretory proteins. The ER is a multifunctional organelle crowded with many enzymes, foldases and chaperones that assist oxidative protein folding and other post-translational modifications which ensure the maintenance of ER homeostasis [1]. In addition, cells have developed different quality control systems in order to ensure that only properly folded proteins are exported through the other compartments of the secretory pathway, the improperly folded proteins being degraded by the proteasome in a process called ER-associated degradation (ERAD) [2]. Intrinsic (genetic mutations, aneuploidy) and extrinsic (environmental disturbances) factors compromise ER homeostasis leading to a situation called ER stress that occurs when the balance between the protein folding demand exceeds that of the ER. In this situation, cells adapt by adjusting their folding capacity through activation of an intracellular signaling pathway known as the unfolded protein response (UPR) (**Figure 1**). Once activated, the UPR outputs can be measured by different methods that are discussed below. Monitoring the UPR outputs through measuring the activation of the different signaling pathways of the UPR represents a powerful and easy tool but may not be enough to mirror ER proteostasis. In this article, we also review the available methods to assess ER homeostasis and stress as well as their use in biological research. Our recommendation is to test different outputs including signaling pathways, ER morphology, ER calcium flux in addition to assessing changes in the ER redox state to ensure the production of a proper representation of the ER functionality.

APPROACHES TO ASSESS ER STRESS

1. THE UNFOLDED PROTEIN RESPONSE

The UPR is transduced by three ER transmembrane sensor proteins (PERK, ATF6α and IRE1α), through their luminal domains they are able to monitor and sense the protein folding status of the ER, then they signal through their cytosolic domain either directly through

specific catalytic activities or select post-translational processing (**Figure 1**). UPR signaling aims at alleviating stress, however if homeostasis cannot be restored the UPR activates cell death pathways [3]. Hence, ER stress and the UPR play an important role in physiology and in the development of numerous diseases.

1.1. The IRE1α arm

IRE1α (referred to IRE1 hereafter) is the most conserved sensor of the UPR, present from yeast to human. IRE1 is a type I transmembrane protein with a lumenal domain that senses misfolded proteins and a cytosolic domain comprising two catalytic activities, a serine/threonine kinase and an endoribonuclease (RNase) (**Figure 1**). Accumulation of misfolded proteins in the ER leads to IRE1 dimerization and trans-autophosphorylation. IRE1 activation can be directly measured by assessing the phosphorylation state at Serines724 or 729 which are phosphorylated upon its activation, antibodies specific for the phosphorylated IRE1 are available commercially (S724) or upon request (S729) (**Table 1**). Because IRE1 is poorly abundant, it is useful to concentrate the protein by immunoprecipitation (IP) prior to immunoblotting (IB) (IP-IB). Alternatively, a Phostag-based western blot approach, can be used. In particular, this method allows a direct visualization and quantitation of IRE1 signalling in various conditions [4] (Supplementary protocol 1). Moreover, IRE1 oligomerization state can be tested to measure its activity, for instance using the sfGFP-IRE1 construct in which the superfolder green fluorescent protein (sfGFP) is N-terminally fused to the luminal domain of IRE1 (**Table 2**) [5].

IRE1α phosphorylation causes a conformational change leading to the activation of the RNase domain which in turn leads to the excision of a 26-nt intron from the XBP1 mRNA. The 5' and 3' fragments are then ligated by the tRNA ligase RTCB [6] This non-conventional splicing shifts the open reading frame on the mRNA resulting in the translation into an active transcription factor XPB1s [7]. The abundance of XBP1s can be measured by using PCR with primers flanking the intron (**Table 3**). XBP1u (unspliced) amplicons migrate on agarose gel (3 or 4%) around 476bp while XBP1s amplicons' mobility is faster (450bp). Alternatively, because the 26nt intron amplicon contains a Pst1 cleavage site, digestion with

Pst1 after PCR yields better separation of XBP1u/s with XBP1u producing two fragment of ~186 and ~290 bp whereas the XBP1s corresponds to an amplicon of ~450bp (Supplementary protocol 2). In addition, is also possible to measure XBP1s mRNA by qPCR using primers that only recognize XBP1 spliced version (**Table3**) [8].

A genetic method to monitor XBP1 mRNA splicing has been developed by fusing XBP1 sequence to venus, a GFP variant or to luciferase (**Table 2**). Venus/luciferase was cloned downstream of the 26-nt ER stress-specific intron of human XBP1. Similar to endogenous XBP1, upon ER stress the frame shift allows expression of the chimeric XBP1-venus/luciferase mRNA [9], which can in turn be detected using either microscopy or luciferase-based light emission thus making it a suitable method to monitor Xbp1 splicing *in-vitro* and *in-vivo* models including mouse, worms and flies. Another Xbp1-Venus variant was developed (F-XBP1ΔDBD-venus) which lacks the DNA binding domain of Xbp1. Because it is unable to bind DNA and mainly localize to the cytosol, F-XBP1ΔDBD-venus is recommended in experiments that requires overexpression of the reporter without interfering in a dominant negative way with induction of UPR target genes. At last, the expression of the XBP1s protein can be measured using western blotting approaches (**Table 1**).

Once in the nucleus, XBP1s regulate the transcription of subset of genes that have a cis-acting element called unfolded protein response element (UPRE/[TGACGTGG/A]). The expression of these target genes can be monitored using real-time PCR and primers can be found in **Table 3**. IRE1 RNase can also regulate the stability of different RNAs through endonucleolytic cleavage of either mRNAs encoding for ER targeted proteins, mRNAs that localize to the ER membrane or miRNAs in a mechanism called Regulated IRE1-Dependent Decay (RIDD) of RNA [10-12]. RNA stability can be assayed by measuring the IRE1-dependent decay and is usually assessed after pulsing cells with the transcription inhibitor actinomycin D in the presence and absence of ER stressor. As a control, RNAi-mediated silencing of IRE1 is usually used in cells lacking functional XBP1 [11] or alternatively, the IRE1 RNase activity can be blocked using select pharmacological inhibitors (**Table 2**). For assaying the cleavage of cellular RNA *in vitro*, recombinant IRE1 is incubated with total RNA for 2hrs. One good negative control for this reaction is the use of heat-denatured IRE1. This

is followed by qRT-PCR with primers flanking regions of potential cleavage sites and then the relative mRNA levels of each reaction is normalized to housekeeping gene such as GAPDH. Examples of RIDD target mRNA and corresponding primers are listed in **Table 1**.

Finally, IRE1 was shown to lead to the activation of JNK1 through interacting with TRAF2, an adaptor protein that couples plasma membrane receptors to c-Jun NH2-terminal kinase (JNK) activation. JNK1 phosphorylation can be tested using western blot, as a surrogate marker of its activation, using phospho-JNK1 antibodies (**Table 1**) [13].

1.2. The PERK arm

PERK is a type I transmembrane protein which is functionally and structurally related to IRE1 (**Figure 1**). The ER luminal portion of PERK contains a stress-sensing domain and the cytoplasmic portion of PERK has a protein kinase domain that is activated when PERK dimerize and/or oligomerize in stressed cells [14, 15]. PERK activity is mainly linked to global translation inhibition, anti-oxidative response and mitochondrial bioenergetics demands [16-18]. Once PERK is activated, it phosphorylates the α-subunit of the eukaryotic translation initiation factor 2 alpha (eIF2α) to attenuate global translation and to reduce ER-lumen protein load [16]. To measure PERK activation, PERK and eIF2α phosophorylation status can be detected using antibodies for total and phospho-specific proteins (**Table 1**). We must note that proper controls (such as the use of PERK inhibitors) should be carried when assaying eIF2α phosphorylation as it can also be phosphorylated in PERK independent way through GCN2, PKR and HRI. Notably, since phospho-PERK specific antibodies do not work well in many cell types and because of the low abundancy of PERK protein, the anti-total PERK can be used to measure the band shift obtained upon Thapsigargin (Tg), tunicamycin (Tm) or dithiothreitol (DTT) treatments using western blot [4]. Alternatively, immunoprecipitating PERK before immunoblotting (IP-IB) with anti-phospho-PERK antibodies increases the efficiency of this method.

Although cap-dependent translation is inhibited, translation of certain transcripts is increased. In particular, transcription factor such as ATF4 is selectively induced in response to eIF2α phosphorylation [19, 20]. ATF4 acts as a transcriptional activator of various pro-

survival genes including many ER chaperones and antioxidative factors [21]. Interestingly, ATF4 target genes also include well-known factors that are associated with ER stress-induced apoptosis such as CHOP/GADD153 and NOXA. The expression of ATF4 can be measured using western blotting (**Table 1**) and the expression of its target genes can be evaluated using real-time PCR (**Tables 3**).

In addition, since it is well established that other eIF2α kinases exist, other controls should be included to confirm PERK dependent eIF2α phosphorylation. Other methods to measure PERK activity, could be testing both mRNA and protein levels of downstream targets such as ATF4 and CHOP. PERK activation induces the phosphorylation of the transcription factor NRF2. Normally, NRF2 is kept in check by interaction with the protein KEAP1. Upon phosphorylation by PERK, NRF2 is liberated from KEAP1 and translocates to the nucleus where it activates the transcription of genes encoding antioxidant proteins [22]. Thus, NRF2 protein levels and its target genes could represent a good strategy to test PERK activity. Finally, translational attenuation can be useful tool to test PERK activation by taking advantages from metabolic pulse labelling of newly synthesized proteins and polyribosome profiling [16] (Supplementary protocol 3). Pharmacological inhibition of PERK can be achieved using specific compounds as described in **Table 2.**

1.3 The ATF6 arm

ATF6 is a 90kDa type II single pass transmembrane protein that is present in two variants in mammalian cells -ATF6α and ATF6β (Figure 1). During ER stress, ATF6 translocate from the ER-to Golgi where it gets cleaved by two serine-proteases (S1P and S2P) to generate a 50kDa active basic-leucine zipper (bZip) transcriptional factor (ATF6f) [23]. ATF6α activation can be monitored using western blot and specific antibodies to the C-terminus of the protein (**Table 1**). Upon ER stress ATF6 and ATF6f can be resolved as 90 kDa and 55 kDa proteins by SDS-PAGE, respectively. Alternatively, cells can be transfected with a 3xFLAG-human ATF6α plasmid (Addgene, Plasmid #11975) (**Table 2**) and the activation (processing) detected using anti-FLAG antibodies (**Table 2**). Of note, it is important to ensure the

amounts of plasmid transfected are appropriate for each cell type studied as too much of ATF6 expression promotes its activation.

In the nucleus, ATF6f promotes transcription of UPR target genes through binding of three different consensus sequences: (ERSE)-I (CCAAT-N9-CCACG/A), ERSE-II (ATTGG-N1-CCACG) and the UPRE [24, 25]. ATF6f transcriptional activity can be assayed by measuring the expression and transcription of most of its cognate targets [26-28]. The expression of these target genes can be monitored at the transcript level using real-time PCR (**Table 3**) or using western blot with specific antibodies (**Table 1**). Another way to evaluate the ATF6f activity is by introducing cells with a luciferase construct, that was made by adding five repetitions of a specific binding sequence for ATF6f upstream to the luciferase gene (p5xATF6-GL3, Addgene, Plasmid #11976) [25]. This construct is highly specific for ATF6 activity allowing researchers to measure ATF6 activation both in untreated conditions and during ER stress induction. In vivo, the ATF6 activity can be monitored using the ERSE-LacZ mouse model that was constructed by using LacZ reporter gene driven by the GRP78 promoter [29]. As a control and in order to control specificity of this system it is important to use the ERSE model lacking the GRP78 promoter [29]. The selective pharmacological inhibition or activation of ATF6 can be achieved using specific drugs as described in **Table 2**.

2. MONITORING CHANGES IN THE ER REDOX STATE

ER unique redox metabolism supports disulfide bond formation in protein substrates. These are catalyzed by the FAD containing ER oxidase (ERO1), and proteins from the disulfide isomerase (PDI) family, yielding to H_2O_2 as a by-product [30-34]. Poorly defined ER reducing pathways are also needed to reduce non-native disulfides and terminally unfolded proteins, thus maintaining/restoring ER homeostasis. To function, these are linked to the cytosolic reduction pathways, namely the glutathione (GSH) and the thioredoxin (TXN) pathways. While the way TXN pathway operates in ER reduction remains enigmatic, GSH is imported in the ER where it can reduce PDI and reset ERO1 activity, both of which shall help relieve ER stress conditions. Yet, irremediable misfolded protein accumulation may engage

futile cycles of oxidation and reduction, triggering H_2O_2 production and exhausting GSH pools [35]. The UPR control of few redox enzymes and the sensitivity of the UPR to redox cues further highlight the reciprocal interconnection linking ER stress to redox metabolism [36].

Monitoring ER redox parameters shall thus be informative to rationalize if and how they deviate during ER stress, which could then be used as independent measures of ER health. As non-proteinaceous molecules, monitoring GSH and H_2O_2 ER redox state and levels is challenging. It benefited from the development of genetically-encoded redox sensitive fluorescent proteins which dynamically measure, in living cells and in a given compartment, the redox state of specific redox couples [37-41]. Stemming from the initial work on the first redox sensitive YFP, rxYFP [42], the repertoire of these redox biosensors now includes a family of ratiometric roGFPs (for reduction- oxidation sensitive GFP) [37, 43]. Mechanistically, both rxYFP and roGFPs surface-expose two redox-active cysteines, located close to the fluorophore whose protonation status is then affected by the structural modifications brought about by the reversible cysteine oxidation. Consequently, in the oxidized probe, the excitation peak at 400 nm increases at the expense of the peak at 490 nm. The ratio of fluorescence after excitation at these two wavelengths reports on the redox state of the probe and thus on the redox potential of the equilibrating couple, somehow independently of the probe concentration. Ratiometric measurement of roGFPs redox status can be determined in living cells by FACS, confocal microscopes or plate readers and by non-reducing western-blotting, after quenching of free cysteines with alkylating agents and cell lysis. **(Table 1** and **Table 2)**.

rxYFP/roGFPs equilibrates with the GSH/GSSG couple, a reaction enhanced by fusing the probes to the glutaredoxin-1 (GRX) enzyme [44-46]. Targeted to the ER, (GRX1-) rxYFP/roGFPs locally reports on the reduction potential of GSH (E_{GSH}), which integrates both the extent of ERO1-PDI dependent oxidation of GSH and of its ER transport. Nevertheless, measuring E_{GSH} in the ER with rxYFP/roGFPs should be taken cautiously. First, as targets of ERO1-PDI, rxYFP/roGFPs may also directly report on their activity independently of GSH [47, 48]. Second, the probe may wrongly report on ER redox

modulation if mistargeted or refluxed from the ER to the cytosol upon stress [49]. A solution is to tether the probe to the ER membrane [40]. Third, it is critical to consider the range of redox potentials the probe linearly reports on, which typically lies within +/- 40 mV from the probe midpoint redox potential [50]. As the ER is more oxidizing than the cytosol, ER-specific probes with shifted midpoint redox potentials have been developed [43] by inserting either a leucine or a glutamic acid at GFP position 147. Because these probes have an intrinsically lower fluorescence, FLIM imaging, based on the distinct fluorescence life time between the reduced and oxidized probe [51], and insertion of additional GFP superfolder mutations have been worked out for these variants [52] [53]. Fusing roGFP probes to peroxide sensors instead of GRX1 shifts the probe specificity toward H_2O_2 detection([54-56]. Targeted to the ER, these probes however also behave as PDI substrate and thus do not strictly report on ER H_2O_2 production [57]. To overcome this caveat, several modifications of disulphide-based reporters and protocols were suggested [57, 58]. A better way to solve this issue would be the development of disulphide independent ER probes that are actively being searched for [59, 60]. Peroxide probes will however never report on H_2O_2 levels as dynamically and accurately as GSH/GSSG reporting probes. Indeed, the H_2O_2 / H_2O redox couple being unproductive in the reduction reaction, the probe redox state will also depend on *in situ* reductase activities, which will differ among cellular compartments. Alternatively, irreversibly oxidized probes oxidation will not provide dynamic monitoring. Quantifying H_2O_2 ER production thus faces important intrinsic challenges. Finally, directly reporting the redox state of ER proteins, especially endogenous ones, shall provide a complementary and necessary approach to map redox events triggered by ER stress. Different technics are currently carried out ranging from non-reducing western blotting to elaborated mass-spectrometry analyses [61]. Proteins to be followed should include ERO1 and PDI family members, but also disulfide containing substrates to scrutinize oxidative folding efficiency.

3. MEASURING CALCIUM DISTRIBUTION:

Although it is considered mainly as a factory for protein folding, the ER is the largest Ca^{2+} store in the cell. Calcium release from this compartment can be monitored using several

chemical and genetic tools. Since the synthesis more than 30 years ago of quin2 then fura2, tens of chemical fluorescent markers of calcium that vary in their Ca2+ dissociation constants (Kd) or Ca2+ response range, excitation/emission wavelengths and spectral shift have been proposed [62-64]. Acetomethoxy (AM) derivatives of these probes allow the dyes to readily enter cells. Once inside, non-specific intracellular esterases cleave the AM groups off, thus trapping the dyes within the cells [65]. These markers have also a very good signal/noise ratio and a large dynamic range. Moreover, they are easy to calibrate and some of them are ratiometric, i.e. that upon binding to calcium, they undergo a shift either in excitation wavelength, emission wavelength, or both, therefore avoid artifacts, for example related to the geometry of the cells. The most used dyes are the fura2 which allows ratiometric measurements, the fluo4 which shows a very good signal/noise ratio and a newer marker the cal520 which is retained longer in the cells (**Table 2**). In the context of the UPR, the genetic indicators of calcium are probably a better choice for calcium measurements since they allow to observe calcium variations over long periods of time, compatible with kinetics of the expression patterns of UPR-target genes induced by UPR-inducing compounds such as Tg or tunicamycin, and which are observed at least 4 hours after treatment[66]. In addition, the large color palette of these calcium indicators available now, makes it easy to observe at the same time, variations in calcium in different compartments.

There are plenty of Genetically Encoded Calcium Indicators (GECIs), which consist in general of a calcium-binding domain (calmodulin or troponin C), fused to one or two fluorescent proteins (FP). These markers can be thus divided into two main groups: single-FP vs. double-FP GECIs (see [67] for review). In the first case, the fluorescence intensity of a circularly permuted or split FP is modulated by calcium binding–dependent changes in the chromophore environment. Single-FP-type GECIs show generally a high dynamic range and because they show narrow excitation and emission spectra, allow to use them with other fluorescent molecules. Double-FP GECIs, rely on the principle of Förster resonance energy transfer (FRET) is that the fluorescence variation of the two FPs allows ratiometric measurements. Indeed, Ca2+ binding to the Ca2+ sensitive element induces a conformational change in the indicator, which modifies the FRET efficiency between the two

FPs, resulting in a change in FP fluorescence intensity. Note that certain single-FP indicators can be used also for ratiometric imaging. The first ER GECIs, such as the YC3er developed as early as 1997, were based on FRET and were subsequently improved to generate D1ER family and others YCer [68-70]. More recently, several groups introducing mutations in calcium binding sites of calmodulin, have developed different types of single-FP GECIer [71]. Among them, our preference is for the CEPIA family (**Table 2**). In our hands, these GECIs show a large dynamic and a very good signal-to-noise ratio.

Although it is interesting to measure calcium in the ER, it is also important to visualize the calcium coming out of the ER. Experiments with chemical fluorophores have shown that calcium release from ER occurred at specific ER sites rich in RInsP3 [72] particularly in areas of contact with mitochondria called MAMs (mitochondria associated membranes). Thus, in order to measure Ca^{2+} release from the ER at subcellular resolution, several GECI have been developed, targeted either to the outer ER membrane , or to the outer mitochondria membrane (**Table 2**) [72, 73].

4. ASSESSING ER STRUCTURE AND FUNCTIONS

The ER is an organelle of many different functions that must be tightly regulated to carry out the proper functions. When there is an increase in protein folding demand, translational inhibition, degradation of unfolded or misfolded proteins, and an increase in the production of chaperones and folding enzymes are part of the adaptive response. In this case the cell must be capable to adjust the morphology, architecture, dimension and molecular composition of specific organelle to meet the increase in protein folding demand. The ER has the plasticity to expand its surface in response to cargo load and in order to increase the expression of resident chaperones and other factors to assist protein folding. The same observation was also documented in the case of B -lymphocytes differentiating into plasma B-cells that need to secrete huge amounts of immunoglobin. Using Electron Microscopy (EM) it was shown that the ER in this case fills all the cytoplasm [74, 75]. The use of EM or the use of immunofluorescence against ER membrane proteins including Calnexin and Sec63 which are powerful methods to assess the size and shape of the ER, do not allow to

follow the kinetics of the morphological change of this organelle [76]. Fluorescent dyes such as the long-chain carbocyanines DiIC16(3) and DiIC18(3), have long been used to monitor the ER morphology in living cells [77]. In most of the above cases measuring ER stress needs either introducing of exogenic proteins or assaying mRNA/Protein levels indirectly. In order to be able to look at protein aggregation during ER stress, a small molecule called Thioflavin T (ThT) was developed. Thioflavin can give us a direct quantifiable measure of ER stress in living cell in Real Time. ThT exhibits enhanced fluorescence when it binds to protein aggregates -particularly β-sheets - and it correlates with the induction of the UPR. ThT can be used in different cell types and responds to different ER stress stimulators. It has an advantage that can be assayed *in-vivo* and in mouse tissue samples without the need to *in-vivo* introduction of an exogenous transgene reporter like measuring the decrease in activity of secreted alkaline phosphatase (SEAP), XBP1-Venus or the Ca^{+2} indicator GLuc. Thus, it makes ThT a more handy technique to rapidly detect and quantify misfolded proteins [78-82]. At last, the ER function in protein biogenesis can be monitored either by measuring the secretion of cargo proteins in the culture medium using western blot (**Table 1**) or by using a secretion reporter with Gaussia luciferase (**Table 2**).

CONCLUSION

No doubt that the ER plays an important function in development and in different diseases. Monitoring the folding state of the ER and to be able to measure and quantify the stress within this organelle is an important feature that will help many labs that are interested to monitor the function of the ER and the subsequent ER stress response in different disease models. We believe that the experimental approaches reviewed here should help researcher to better evaluate ER protein folding stress *in-vitro* and *in-vivo*. As mentioned before, we highly recommend not to rely on one assay for this task and to try and test as many outputs as possible.

References

1. Rapoport, T.A., *Protein translocation across the eukaryotic endoplasmic reticulum and bacterial plasma membranes.* Nature, 2007. **450**(7170): p. 663-9.
2. Vembar, S.S. and J.L. Brodsky, *One step at a time: endoplasmic reticulum-associated degradation.* Nat Rev Mol Cell Biol, 2008. **9**(12): p. 944-57.
3. Oyadomari, S., et al., *Targeted disruption of the Chop gene delays endoplasmic reticulum stress-mediated diabetes.* J Clin Invest, 2002. **109**(4): p. 525-32.
4. Qi, L., L. Yang, and H. Chen, *Detecting and quantitating physiological endoplasmic reticulum stress.* Methods Enzymol, 2011. **490**: p. 137-46.
5. Ghosh, R., et al., *Allosteric inhibition of the IRE1alpha RNase preserves cell viability and function during endoplasmic reticulum stress.* Cell, 2014. **158**(3): p. 534-48.
6. Jurkin, J., et al., *The mammalian tRNA ligase complex mediates splicing of XBP1 mRNA and controls antibody secretion in plasma cells.* EMBO J, 2014. **33**(24): p. 2922-36.
7. Calfon, M., et al., *IRE1 couples endoplasmic reticulum load to secretory capacity by processing the XBP-1 mRNA.* Nature, 2002. **415**(6867): p. 92-6.
8. van Schadewijk, A., et al., *A quantitative method for detection of spliced X-box binding protein-1 (XBP1) mRNA as a measure of endoplasmic reticulum (ER) stress.* Cell Stress Chaperones, 2012. **17**(2): p. 275-9.
9. Iwawaki, T., et al., *A transgenic mouse model for monitoring endoplasmic reticulum stress.* Nat Med, 2004. **10**(1): p. 98-102.
10. Hollien, J. and J.S. Weissman, *Decay of endoplasmic reticulum-localized mRNAs during the unfolded protein response.* Science, 2006. **313**(5783): p. 104-7.
11. Hollien, J., et al., *Regulated Ire1-dependent decay of messenger RNAs in mammalian cells.* J Cell Biol, 2009. **186**(3): p. 323-31.
12. Maurel, M., et al., *Controlling the unfolded protein response-mediated life and death decisions in cancer.* Semin Cancer Biol, 2015. **33**: p. 57-66.
13. Urano, F., et al., *Coupling of stress in the ER to activation of JNK protein kinases by transmembrane protein kinase IRE1.* Science, 2000. **287**(5453): p. 664-6.

14. Carrara, M., et al., *Noncanonical binding of BiP ATPase domain to Ire1 and Perk is dissociated by unfolded protein CH1 to initiate ER stress signaling.* Elife, 2015. **4**.
15. Carrara, M., et al., *Crystal structures reveal transient PERK luminal domain tetramerization in endoplasmic reticulum stress signaling.* EMBO J, 2015. **34**(11): p. 1589-600.
16. Harding, H.P., Y. Zhang, and D. Ron, *Protein translation and folding are coupled by an endoplasmic-reticulum-resident kinase.* Nature, 1999. **397**(6716): p. 271-4.
17. Bobrovnikova-Marjon, E., et al., *PERK promotes cancer cell proliferation and tumor growth by limiting oxidative DNA damage.* Oncogene, 2010. **29**(27): p. 3881-95.
18. Balsa, E., et al., *ER and Nutrient Stress Promote Assembly of Respiratory Chain Supercomplexes through the PERK-eIF2alpha Axis.* Mol Cell, 2019. **74**(5): p. 877-890 e6.
19. Lu, P.D., H.P. Harding, and D. Ron, *Translation reinitiation at alternative open reading frames regulates gene expression in an integrated stress response.* J Cell Biol, 2004. **167**(1): p. 27-33.
20. Lu, P.D., et al., *Cytoprotection by pre-emptive conditional phosphorylation of translation initiation factor 2.* EMBO J, 2004. **23**(1): p. 169-79.
21. Avivar-Valderas, A., et al., *PERK integrates autophagy and oxidative stress responses to promote survival during extracellular matrix detachment.* Mol Cell Biol, 2011. **31**(17): p. 3616-29.
22. Cullinan, S.B. and J.A. Diehl, *PERK-dependent activation of Nrf2 contributes to redox homeostasis and cell survival following endoplasmic reticulum stress.* J Biol Chem, 2004. **279**(19): p. 20108-17.
23. Ye, J., et al., *ER stress induces cleavage of membrane-bound ATF6 by the same proteases that process SREBPs.* Mol Cell, 2000. **6**(6): p. 1355-64.
24. Kokame, K., H. Kato, and T. Miyata, *Identification of ERSE-II, a new cis-acting element responsible for the ATF6-dependent mammalian unfolded protein response.* J Biol Chem, 2001. **276**(12): p. 9199-205.

25. Wang, Y., et al., *Activation of ATF6 and an ATF6 DNA binding site by the endoplasmic reticulum stress response.* J Biol Chem, 2000. **275**(35): p. 27013-20.
26. Adachi, Y., et al., *ATF6 is a transcription factor specializing in the regulation of quality control proteins in the endoplasmic reticulum.* Cell Struct Funct, 2008. **33**(1): p. 75-89.
27. Yamamoto, K., et al., *Induction of liver steatosis and lipid droplet formation in ATF6alpha-knockout mice burdened with pharmacological endoplasmic reticulum stress.* Mol Biol Cell, 2010. **21**(17): p. 2975-86.
28. Maiuolo, J., et al., *Selective activation of the transcription factor ATF6 mediates endoplasmic reticulum proliferation triggered by a membrane protein.* Proc Natl Acad Sci U S A, 2011. **108**(19): p. 7832-7.
29. Mao, C., et al., *In vivo regulation of Grp78/BiP transcription in the embryonic heart: role of the endoplasmic reticulum stress response element and GATA-4.* J Biol Chem, 2006. **281**(13): p. 8877-87.
30. Gross, E., et al., *Generating disulfides enzymatically: reaction products and electron acceptors of the endoplasmic reticulum thiol oxidase Ero1p.* Proc Natl Acad Sci U S A, 2006. **103**(2): p. 299-304.
31. Tu, B.P. and J.S. Weissman, *The FAD- and O(2)-dependent reaction cycle of Ero1-mediated oxidative protein folding in the endoplasmic reticulum.* Mol Cell, 2002. **10**(5): p. 983-94.
32. Bertoli, G., et al., *Two conserved cysteine triads in human Ero1alpha cooperate for efficient disulfide bond formation in the endoplasmic reticulum.* J Biol Chem, 2004. **279**(29): p. 30047-52.
33. Frand, A.R. and C.A. Kaiser, *The ERO1 gene of yeast is required for oxidation of protein dithiols in the endoplasmic reticulum.* Mol Cell, 1998. **1**(2): p. 161-70.
34. Pollard, M.G., K.J. Travers, and J.S. Weissman, *Ero1p: a novel and ubiquitous protein with an essential role in oxidative protein folding in the endoplasmic reticulum.* Mol Cell, 1998. **1**(2): p. 171-82.
35. Malhotra, J.D., et al., *Antioxidants reduce endoplasmic reticulum stress and improve protein secretion.* Proc Natl Acad Sci U S A, 2008. **105**(47): p. 18525-30.

36. Eletto, D., et al., *Redox controls UPR to control redox.* J Cell Sci, 2014. **127**(Pt 17): p. 3649-58.
37. Dooley, C.T., et al., *Imaging dynamic redox changes in mammalian cells with green fluorescent protein indicators.* J Biol Chem, 2004. **279**(21): p. 22284-93.
38. Hanson, G.T., et al., *Investigating mitochondrial redox potential with redox-sensitive green fluorescent protein indicators.* J Biol Chem, 2004. **279**(13): p. 13044-53.
39. Merksamer, P.I., A. Trusina, and F.R. Papa, *Real-time redox measurements during endoplasmic reticulum stress reveal interlinked protein folding functions.* Cell, 2008. **135**(5): p. 933-47.
40. Ponsero, A.J., et al., *Endoplasmic Reticulum Transport of Glutathione by Sec61 Is Regulated by Ero1 and Bip.* Mol Cell, 2017. **67**(6): p. 962-973 e5.
41. Ezerina, D., B. Morgan, and T.P. Dick, *Imaging dynamic redox processes with genetically encoded probes.* J Mol Cell Cardiol, 2014. **73**: p. 43-9.
42. Ostergaard, H., C. Tachibana, and J.R. Winther, *Monitoring disulfide bond formation in the eukaryotic cytosol.* J Cell Biol, 2004. **166**(3): p. 337-45.
43. Lohman, J.R. and S.J. Remington, *Development of a family of redox-sensitive green fluorescent protein indicators for use in relatively oxidizing subcellular environments.* Biochemistry, 2008. **47**(33): p. 8678-88.
44. Gutscher, M., et al., *Real-time imaging of the intracellular glutathione redox potential.* Nat Methods, 2008. **5**(6): p. 553-9.
45. Bjornberg, O., H. Ostergaard, and J.R. Winther, *Mechanistic insight provided by glutaredoxin within a fusion to redox-sensitive yellow fluorescent protein.* Biochemistry, 2006. **45**(7): p. 2362-71.
46. Birk, J., et al., *Green fluorescent protein-based monitoring of endoplasmic reticulum redox poise.* Front Genet, 2013. **4**: p. 108.
47. Tsunoda, S., et al., *Intact protein folding in the glutathione-depleted endoplasmic reticulum implicates alternative protein thiol reductants.* Elife, 2014. **3**: p. e03421.
48. Avezov, E., et al., *Retarded PDI diffusion and a reductive shift in poise of the calcium depleted endoplasmic reticulum.* BMC Biol, 2015. **13**: p. 2.

49. Igbaria, A., et al., *Chaperone-Mediated Reflux of Secretory Proteins to the Cytosol During Endoplasmic Reticulum Stress.* bioRxiv, 2019: p. 562306.
50. Meyer, A.J. and T.P. Dick, *Fluorescent protein-based redox probes.* Antioxid Redox Signal, 2010. **13**(5): p. 621-50.
51. Avezov, E., et al., *Lifetime imaging of a fluorescent protein sensor reveals surprising stability of ER thiol redox.* J Cell Biol, 2013. **201**(2): p. 337-49.
52. Zhang, J., et al., *Secretory kinase Fam20C tunes endoplasmic reticulum redox state via phosphorylation of Ero1alpha.* EMBO J, 2018. **37**(14).
53. Hoseki, J., et al., *Development of a stable ERroGFP variant suitable for monitoring redox dynamics in the ER.* Biosci Rep, 2016. **36**(2).
54. Bilan, D.S. and V.V. Belousov, *New tools for redox biology: From imaging to manipulation.* Free Radic Biol Med, 2017. **109**: p. 167-188.
55. Morgan, B., et al., *Real-time monitoring of basal H2O2 levels with peroxiredoxin-based probes.* Nat Chem Biol, 2016. **12**(6): p. 437-43.
56. Gutscher, M., et al., *Proximity-based protein thiol oxidation by H2O2-scavenging peroxidases.* J Biol Chem, 2009. **284**(46): p. 31532-40.
57. Melo, E.P., et al., *TriPer, an optical probe tuned to the endoplasmic reticulum tracks changes in luminal H2O2.* BMC Biol, 2017. **15**(1): p. 24.
58. Ramming, T., et al., *GPx8 peroxidase prevents leakage of H2O2 from the endoplasmic reticulum.* Free Radic Biol Med, 2014. **70**: p. 106-16.
59. Gao, C., et al., *Endoplasmic Reticulum-Directed Ratiometric Fluorescent Probe for Quantitive Detection of Basal H2O2.* Anal Chem, 2017. **89**(23): p. 12945-12950.
60. Xiao, H., et al., *Simultaneous fluorescence imaging of hydrogen peroxide in mitochondria and endoplasmic reticulum during apoptosis.* Chem Sci, 2016. **7**(9): p. 6153-6159.
61. Chiappetta, G., et al., *Proteome screens for Cys residues oxidation: the redoxome.* Methods Enzymol, 2010. **473**: p. 199-216.
62. Bootman, M.D., et al., *Ca2+-sensitive fluorescent dyes and intracellular Ca2+ imaging.* Cold Spring Harb Protoc, 2013. **2013**(2): p. 83-99.

63. Minta, A., J.P. Kao, and R.Y. Tsien, *Fluorescent indicators for cytosolic calcium based on rhodamine and fluorescein chromophores.* J Biol Chem, 1989. **264**(14): p. 8171-8.
64. Paredes, R.M., et al., *Chemical calcium indicators.* Methods, 2008. **46**(3): p. 143-51.
65. Oakes, S.G., et al., *Incomplete hydrolysis of the calcium indicator precursor fura-2 pentaacetoxymethyl ester (fura-2 AM) by cells.* Anal Biochem, 1988. **169**(1): p. 159-66.
66. Shinjo, S., et al., *Comparative analysis of the expression patterns of UPR-target genes caused by UPR-inducing compounds.* Biosci Biotechnol Biochem, 2013. **77**(4): p. 729-35.
67. Suzuki, J., K. Kanemaru, and M. Iino, *Genetically Encoded Fluorescent Indicators for Organellar Calcium Imaging.* Biophys J, 2016. **111**(6): p. 1119-1131.
68. Palmer, A.E., et al., *Bcl-2-mediated alterations in endoplasmic reticulum Ca2+ analyzed with an improved genetically encoded fluorescent sensor.* Proc Natl Acad Sci U S A, 2004. **101**(50): p. 17404-9.
69. Tang, S., et al., *Design and application of a class of sensors to monitor Ca2+ dynamics in high Ca2+ concentration cellular compartments.* Proc Natl Acad Sci U S A, 2011. **108**(39): p. 16265-70.
70. Whitaker, M., *Genetically encoded probes for measurement of intracellular calcium.* Methods Cell Biol, 2010. **99**: p. 153-82.
71. Suzuki, J., et al., *Imaging intraorganellar Ca2+ at subcellular resolution using CEPIA.* Nat Commun, 2014. **5**: p. 4153.
72. Csordas, G., et al., *Imaging interorganelle contacts and local calcium dynamics at the ER-mitochondrial interface.* Mol Cell, 2010. **39**(1): p. 121-32.
73. Bannai, H., et al., *Dissection of Local Ca2+ Signals in Cultured Cells by Membrane-targeted Ca2+ Indicators.* J Vis Exp, 2019(145).
74. van Anken, E., et al., *Sequential waves of functionally related proteins are expressed when B cells prepare for antibody secretion.* Immunity, 2003. **18**(2): p. 243-53.

75. Federovitch, C.M., D. Ron, and R.Y. Hampton, *The dynamic ER: experimental approaches and current questions.* Curr Opin Cell Biol, 2005. **17**(4): p. 409-14.
76. Schuck, S., et al., *Membrane expansion alleviates endoplasmic reticulum stress independently of the unfolded protein response.* J Cell Biol, 2009. **187**(4): p. 525-36.
77. Terasaki, M., L.B. Chen, and K. Fujiwara, *Microtubules and the endoplasmic reticulum are highly interdependent structures.* J Cell Biol, 1986. **103**(4): p. 1557-68.
78. Sigurdsson, E.M., *Histological staining of amyloid-beta in mouse brains.* Methods Mol Biol, 2005. **299**: p. 299-308.
79. Lindgren, M., K. Sorgjerd, and P. Hammarstrom, *Detection and characterization of aggregates, prefibrillar amyloidogenic oligomers, and protofibrils using fluorescence spectroscopy.* Biophys J, 2005. **88**(6): p. 4200-12.
80. Naiki, H., et al., *Fluorometric determination of amyloid fibrils in vitro using the fluorescent dye, thioflavin T1.* Anal Biochem, 1989. **177**(2): p. 244-9.
81. Vassar, P.S. and C.F. Culling, *Fluorescent stains, with special reference to amyloid and connective tissues.* Arch Pathol, 1959. **68**: p. 487-98.
82. Beriault, D.R. and G.H. Werstuck, *Detection and quantification of endoplasmic reticulum stress in living cells using the fluorescent compound, Thioflavin T.* Biochim Biophys Acta, 2013. **1833**(10): p. 2293-301.
83. Tang, C.-H.A., et al., *Phosphorylation of IRE1 at S729 regulates RIDD in B cells and antibody production after immunization.* The Journal of Cell Biology, 2018. **217**(5): p. 1739-1755.
84. Brunsing, R., et al., *B- and T-cell development both involve activity of the unfolded protein response pathway.* J Biol Chem, 2008. **283**(26): p. 17954-61.
85. Acosta-Alvear, D., et al., *XBP1 controls diverse cell type- and condition-specific transcriptional regulatory networks.* Mol Cell, 2007. **27**(1): p. 53-66.
86. Lee, A.H., N.N. Iwakoshi, and L.H. Glimcher, *XBP-1 regulates a subset of endoplasmic reticulum resident chaperone genes in the unfolded protein response.* Mol Cell Biol, 2003. **23**(21): p. 7448-59.

87. Shen, X., et al., *Complementary signaling pathways regulate the unfolded protein response and are required for C. elegans development.* Cell, 2001. **107**(7): p. 893-903.
88. Yoshida, H., et al., *XBP1 mRNA is induced by ATF6 and spliced by IRE1 in response to ER stress to produce a highly active transcription factor.* Cell, 2001. **107**(7): p. 881-91.
89. Han, D., et al., *IRE1alpha kinase activation modes control alternate endoribonuclease outputs to determine divergent cell fates.* Cell, 2009. **138**(3): p. 562-75.
90. Moore, K. and J. Hollien, *Ire1-mediated decay in mammalian cells relies on mRNA sequence, structure, and translational status.* Mol Biol Cell, 2015. **26**(16): p. 2873-84.
91. Lerner, A.G., et al., *IRE1alpha induces thioredoxin-interacting protein to activate the NLRP3 inflammasome and promote programmed cell death under irremediable ER stress.* Cell Metab, 2012. **16**(2): p. 250-64.
92. Upton, J.P., et al., *IRE1alpha cleaves select microRNAs during ER stress to derepress translation of proapoptotic Caspase-2.* Science, 2012. **338**(6108): p. 818-22.
93. Korennykh, A.V., et al., *The unfolded protein response signals through high-order assembly of Ire1.* Nature, 2009. **457**(7230): p. 687-93.
94. Li, H., et al., *Mammalian endoplasmic reticulum stress sensor IRE1 signals by dynamic clustering.* Proc Natl Acad Sci U S A, 2010. **107**(37): p. 16113-8.
95. Harrington, P.E., et al., *Unfolded Protein Response in Cancer: IRE1alpha Inhibition by Selective Kinase Ligands Does Not Impair Tumor Cell Viability.* ACS Med Chem Lett, 2015. **6**(1): p. 68-72.
96. Cross, B.C., et al., *The molecular basis for selective inhibition of unconventional mRNA splicing by an IRE1-binding small molecule.* Proc Natl Acad Sci U S A, 2012. **109**(15): p. E869-78.
97. Papandreou, I., et al., *Identification of an Ire1alpha endonuclease specific inhibitor with cytotoxic activity against human multiple myeloma.* Blood, 2011. **117**(4): p. 1311-4.

98. Mimura, N., et al., *Blockade of XBP1 splicing by inhibition of IRE1alpha is a promising therapeutic option in multiple myeloma.* Blood, 2012. **119**(24): p. 5772-81.
99. Harding, H.P., et al., *Perk is essential for translational regulation and cell survival during the unfolded protein response.* Mol Cell, 2000. **5**(5): p. 897-904.
100. Rojas-Rivera, D., et al., *When PERK inhibitors turn out to be new potent RIPK1 inhibitors: critical issues on the specificity and use of GSK2606414 and GSK2656157.* Cell Death Differ, 2017. **24**(6): p. 1100-1110.
101. Mahameed, M., et al., *The unfolded protein response modulators GSK2606414 and KIRA6 are potent KIT inhibitors.* Cell Death Dis, 2019. **10**(4): p. 300.
102. Sidrauski, C., et al., *Pharmacological brake-release of mRNA translation enhances cognitive memory.* Elife, 2013. **2**: p. e00498.
103. Axten, J.M., et al., *Discovery of 7-methyl-5-(1-{[3-(trifluoromethyl)phenyl]acetyl}-2,3-dihydro-1H-indol-5-yl)-7H-p yrrolo[2,3-d]pyrimidin-4-amine (GSK2606414), a potent and selective first-in-class inhibitor of protein kinase R (PKR)-like endoplasmic reticulum kinase (PERK).* J Med Chem, 2012. **55**(16): p. 7193-207.
104. Belmont, P.J., et al., *Coordination of growth and endoplasmic reticulum stress signaling by regulator of calcineurin 1 (RCAN1), a novel ATF6-inducible gene.* J Biol Chem, 2008. **283**(20): p. 14012-21.
105. Guan, M., K. Fousek, and W.A. Chow, *Nelfinavir inhibits regulated intramembrane proteolysis of sterol regulatory element binding protein-1 and activating transcription factor 6 in castration-resistant prostate cancer.* FEBS J, 2012. **279**(13): p. 2399-411.
106. Hay, B.A., et al., *Aminopyrrolidineamide inhibitors of site-1 protease.* Bioorg Med Chem Lett, 2007. **17**(16): p. 4411-4.
107. Gallagher, C.M., et al., *Ceapins are a new class of unfolded protein response inhibitors, selectively targeting the ATF6alpha branch.* Elife, 2016. **5**.
108. Grynkiewicz, G., M. Poenie, and R.Y. Tsien, *A new generation of Ca2+ indicators with greatly improved fluorescence properties.* J Biol Chem, 1985. **260**(6): p. 3440-50.
109. Rehberg, M., et al., *A new non-disruptive strategy to target calcium indicator dyes to the endoplasmic reticulum.* Cell Calcium, 2008. **44**(4): p. 386-99.

110. Henderson, M.J., et al., *Monitoring Endoplasmic Reticulum Calcium Homeostasis Using a Gaussia Luciferase SERCaMP.* J Vis Exp, 2015(103).
111. Badr, C.E., et al., *A highly sensitive assay for monitoring the secretory pathway and ER stress.* PLoS One, 2007. **2**(6): p. e571.
112. Roy, G., et al., *Development of a fluorescent reporter system for monitoring ER stress in Chinese hamster ovary cells and its application for therapeutic protein production.* PLoS One, 2017. **12**(8): p. e0183694.
113. Lipson, K.L., et al., *Regulation of insulin biosynthesis in pancreatic beta cells by an endoplasmic reticulum-resident protein kinase IRE1.* Cell Metab, 2006. **4**(3): p. 245-54.
114. Smirnova, N.A., et al., *Development of Neh2-luciferase reporter and its application for high throughput screening and real-time monitoring of Nrf2 activators.* Chem Biol, 2011. **18**(6): p. 752-65.
115. Zhu, C., F.E. Johansen, and R. Prywes, *Interaction of ATF6 and serum response factor.* Mol Cell Biol, 1997. **17**(9): p. 4957-66.
116. Shoulders, M.D., et al., *Stress-independent activation of XBP1s and/or ATF6 reveals three functionally diverse ER proteostasis environments.* Cell Rep, 2013. **3**(4): p. 1279-92.
117. Bright, M.D., et al., *Cleavage of BLOC1S1 mRNA by IRE1 Is Sequence Specific, Temporally Separate from XBP1 Splicing, and Dispensable for Cell Viability under Acute Endoplasmic Reticulum Stress.* Mol Cell Biol, 2015. **35**(12): p. 2186-202.
118. Lhomond, S., et al., *Dual IRE1 RNase functions dictate glioblastoma development.* EMBO Mol Med, 2018. **10**(3).
119. Cai, W., et al., *PMP22 Regulates Self-Renewal and Chemoresistance of Gastric Cancer Cells.* Mol Cancer Ther, 2017. **16**(6): p. 1187-1198.
120. Wu, Q., et al., *Decreased expression of hepatocyte nuclear factor 4alpha (Hnf4alpha)/microRNA-122 (miR-122) axis in hepatitis B virus-associated hepatocellular carcinoma enhances potential oncogenic GALNT10 protein activity.* J Biol Chem, 2015. **290**(2): p. 1170-85.

121. Kaser, A., et al., *XBP1 links ER stress to intestinal inflammation and confers genetic risk for human inflammatory bowel disease.* Cell, 2008. **134**(5): p. 743-56.
122. Thamsen, M., et al., *Small molecule inhibition of IRE1alpha kinase/RNase has anti-fibrotic effects in the lung.* PLoS One, 2019. **14**(1): p. e0209824.
123. Sicari, D., et al., *Mutant p53 improves cancer cells' resistance to endoplasmic reticulum stress by sustaining activation of the UPR regulator ATF6.* Oncogene, 2019.
124. Zhang, K. and R.J. Kaufman, *Identification and characterization of endoplasmic reticulum stress-induced apoptosis in vivo.* Methods Enzymol, 2008. **442**: p. 395-419.
125. Xu, S., et al., *Mesencephalic astrocyte-derived neurotrophic factor (MANF) protects against Abeta toxicity via attenuating Abeta-induced endoplasmic reticulum stress.* J Neuroinflammation, 2019. **16**(1): p. 35.
126. Morita, S., et al., *Targeting ABL-IRE1alpha Signaling Spares ER-Stressed Pancreatic beta Cells to Reverse Autoimmune Diabetes.* Cell Metab, 2017. **25**(4): p. 883-897 e8.
127. Wei, M., et al., *Knockdown of RNF2 induces cell cycle arrest and apoptosis in prostate cancer cells through the upregulation of TXNIP.* Oncotarget, 2017. **8**(3): p. 5323-5338.
128. Sun, S., et al., *Sel1L is indispensable for mammalian endoplasmic reticulum-associated degradation, endoplasmic reticulum homeostasis, and survival.* Proc Natl Acad Sci U S A, 2014. **111**(5): p. E582-91.
129. Paredes, F., et al., *HERPUD1 protects against oxidative stress-induced apoptosis through downregulation of the inositol 1,4,5-trisphosphate receptor.* Free Radic Biol Med, 2016. **90**: p. 206-18.
130. Nishio, N. and K. Isobe, *GADD34-deficient mice develop obesity, nonalcoholic fatty liver disease, hepatic carcinoma and insulin resistance.* Sci Rep, 2015. **5**: p. 13519.
131. Wang, Q., et al., *ERAD inhibitors integrate ER stress with an epigenetic mechanism to activate BH3-only protein NOXA in cancer cells.* Proc Natl Acad Sci U S A, 2009. **106**(7): p. 2200-5.
132. Jais, A., et al., *Heme oxygenase-1 drives metaflammation and insulin resistance in mouse and man.* Cell, 2014. **158**(1): p. 25-40.

133. Lisek, K., et al., *Mutant p53 tunes the NRF2-dependent antioxidant response to support survival of cancer cells.* Oncotarget, 2018. **9**(29): p. 20508-20523.

Antibody	Source	Reactivity	Application	Company/Cat#
IRE1α	Rabbit	H, M	IP[1], IF[1], WB[1], IHC[1]	CST/3294S
IRE1α (B12)	Mouse	M,R,H	IP[1], IF[1], WB[1], IHC[1]	SCBT/sc390960
p-IRE1 pS724	Rabbit	M,R,H	WB[2]	Abcam/ab48187
p-IRE1 pS729	Rabbit	M	WB[1]	Tang et al, [83]
XBP1s (9D11A43)	Mouse	H,M	IF[1], WB[1]	Biolegends/658802
XBP1s (D2C1F)	Mouse	H	WB[2]	CST/12782S
RTCB	Rabbit	H,M	IP[1], IF[1], WB[1], IHC[1]	Ptg/19809-1-AP
PERK (C33E10)	Rabbit	H,M,R,Mk	WB[1]	CST/3192S
PERK (D11A8)	Rabbit	H	IP[2], IF[2], WB[1]	CST/5683S
p-PERK (16F8) (Thr980)	Rabbit	R	WB[3]	CST/3179S
p-PERK (Thr982)	Rabbit	H,M	IP[2], IF[1], WB[2], IHC[1]	Abcam/Ab192591
eIF2a (L57A5)	Mouse	H,M,R,Mk	WB[1]	CST/2103S
p-eIF2a(119A11) (S51)	Rabbit	H,M,R,Mk	WB[2]	CST/3597S
ATF4	mouse	M,R,H	WB[1]	Sigma-aldrich/ WH0000468M1
ATF6 (1-7)	Mouse	H	IP[1], IF[1], WB[1]	Abcam/ab122897
CHOP (L63F7)	Mouse	H,M,R	IP[1], IF[1], WB[1]	CST/2895S
BIP (C50B12)	Rabbit	H,M	WB[1]	CST/3177S
PDIA3 (3G4G7)	Mouse	H,M,R	IP[2], IF[1], WB[1], IHC[1]	Ptg/66423-1-Ig
SAPK/JNK	Rabbit	H,M,R	WB[2]	CST/9252S
p-SAPK/JNK(81E11) (Thr183/Tyr185)	Rabbit	H,M,R	WB[2]	CST/4668S
p-SAPK/JNK(G9) (Thr183/Tyr185)	Mouse	H,M,R	WB[2]	CST/9255S
TXNIP	Mouse	H,M,R	WB[1]	[7, 9, 84-88][7, 9, 83-87][7, 9, 82-86][7, 9, 81-85][7, 9, 81-85][7, 9, 81-85][7, 9, 81-85][7, 9, 81-85][7, 9, 81-85][7, 9, 81-85]MBL/ K0205-3
Insulin (2D11-H5)	Mouse	H,M,R	IP[1], IF[1], WB[1], IHC[1]	SCBT/8033
PRDX4	Rabbit	H,M,R	IP[1], IF[1], WB[1], IHC[1]	Ptg/10703-1-AP

BLOS1	Rabbit	H,M,R	IP[1], IF[1], WB[1], IHC[1]	Ptg/19687-1-AP
MANF	Rabbit	H,M	WB[1]	Bethyl/A305-572A
GADD34/PPP1R15A	Rabbit	H,M,R	IP[1], IF[1], WB[1], IHC[1]	Ptg/10449-1-AP

Table 1: List of antibodies used to assess ER stress by WB, IF, IHC and IP. CST= Cell Signaling Technology, SCBT= Santa Cruz Biotechnology, Ptg=ProteinTech. H=Human, M=Mouse, R=R. Application score: 1= Good, 2=medium, 3= bad.

THE UNFOLDED PROTEIN RESPONSE ASSAYS				
		Method	Notes	Ref
IRE1α	XBP1s	PCR/qPCR/WB/Florescence	DnaJ/Hsp40-like genes, EDEM, p58IPK, ERdj4, HEDJ, protein disulfide isomerase-P5 and RAMP4	[7, 9, 84-88]
	IRE1α Phosphorylation	WB/Phostag	pIRE1a antibodies, Phostag Gels	-
	RIDD	WB/qPCR	RTN4, PRDX4, Galnt2, Gyltl1b, Pdia4 and Blos1 (see Refs for list of genes)	[5, 10, 11, 89, 90]
	miRNA	qPCR	miRNA-17, miRNA-34a, miRNA-96 and miRNA-125b	[91, 92]
	IRE1α Oligomerization	WB/Florescence	sfGFP-IRE1a construct EGFP-IRE1a construct	[5, 93, 94]
	Cell death	WB/Annexin V	CHOP/ pJNK/ TXNIP-NLRP3	[5, 13, 91, 92]
	"ER stress-activated indicator" (ERAI)	Florescence	Transgenic mouse	[9]
IRE1□□ Inhibitors	Kinase and RNAse Inhibitor	WB/qPCR on IRE1α and IRE1α targets.	Compound 18, MKC-3946, MKC-8866, STF-083010, 4μ8c.	[95-98]
PERK	PERK phosphorylation	WB/Phostag	pPERK antibodies, Phostag Gels	[16, 99]
	ATF4 target genes	WB/qPCR	CHOP/GADD153 and Noxa	[19-21]
	eIF2α phosophorylation	WB	peIF2□ antibodies	[16, 99]
	NRF2-KEAP1	WB/qPCR of the NRF2 target genes	GCLC, NQO1	[22]
PERK Inhibitors	phosphorylation inhibitors	WB/qPCR on PERK and its targets	GSK-2606414*, GSK2656157* ISRIB * also known to inhibit RIPK1 and/or cKIT [100, 101]	[102, 103]
	ATF6f localization	WB/Luciferase	p5xATF6-GL3, Plasmid #11976	[25]

		assay		
ATF6	ATF6f target genes	WB/qPCR	GRP78, GRP94, ERp72, PDIA4, SEL1L, OS9, HerpUD and Hyou1	[104]
	ERSE-LacZ model mouse model	Florescence	Transgenic mouse	[29]
ATF6 Inhibitor	ATF6-f transport inhibitor, S1p protease inhibitors.	WB/qPCR on ATF6 protein and ATF6 targets	Ceapins, Nelfinavir PF-429242	[105-107]
ASSESSING THE REDOX STATE OF THE ER				
Redox state of the ER lumen	Assaying the redox state of redox sensitive Fluorescent Proteins	Non reducing WB/ Fluorescence/FACS/Microscopy	eroGFP, ER-rxYFGP, Grx-rxYFP, PDI redox state, ERO1 redox state	[37-41, 43, 45-47, 51, 53]
MEASURING CALCIUM DISTRIBUTION				
	Chemical Indicators	Fluorescent dyes Cytosol :	Fura-2, Fluo3, Fluo4, Calcium Green-1, Indo1, Cal-520, etc…	[62-64, 108]
		ER lumen	Mag-Fura2, Mag-Fluo4, Fluo-4FF, Fluo-5N, Calcium Green-5N, Magnesium Green NTA	
	GECIs	Florescence/Microscopy	CEPIA family, YC family, D1ER and CatchER	[68-70]
	(TED)	Florescence/Microscopy	GFPCES3, Fluo 5N/Ca+2	[109]
	membrane-targeted GECIs	Florescence/Microscopy	OER-GCaMP6f, Lck-GCaMP6f, LcK-RCaMP2	[73]
	Gaussia Luciferase SERCaMP	Luminescence	SERCaMP	[110]
FUNCTIONAL CHANGES				
Morpho	ER size and shape	EM, Fluorescent Microscopy Immunofluorescence	EM, ER-Tracker™, DiIC16(3) and DiIC18(3), PDI, SERCA, GPR78 etc… GFP-Sec63, Calnexin IF	[74, 75]

Function	Secretion	Luciferase assay	Gaussia luciferase	[111]
MISFOLDED PROTEIN AGGREGATION				
	Protein Aggregation	Fluorescence	Thioflavin	[78-82]
THE UNFOLDED PROTEIN RESPONSE GENETICS TOOLS				
		Method	Notes	Ref
IRE1□	Xbp1s	XBP1-venus F-XBP1ΔDBD-venus	monitoring the fluorescence activity of venus in the nucleus	[7, 9, 84-88]
	IRE1α RNAse activity	RFP-GFP fusion	Flow Cytometry	[112]
	IRE1□ Oligomerization	WB/Florescence	sfGFP-IRE1α construct EGFP-IRE1α construct	[5, 93, 94]
	IRE1α	Transfection	IRE1α KA-pcDNA3.EGFP IRE1α-pcDNA3.EGFP	[113]
PERK	NRF2-KEAP1	Luciferase assay	Neh2-luciferase to monitor drug-induced Nrf2 stabilizationin	[114]
ATF6	ATF6f localization	Luciferase assay	p5xATF6-GL3, Plasmid #11976	[25]
	ATF6 localization	Immufluorescence	p5xFLAG-ATF6, Plasmid #11974	[115]
	ATF6f localization	Immunofluorescence	pCGN-ATF6 (1-373), Plasmid #27173 pCGN-ATF6 (1-373)m, Plasmid #27174	[25]
	ATF6 nuclear localization	Western blot/Immunofluorescence, Selective ATF6f induction	DHFR:ATF6	[116]
ASSESSING THE REDOX STATE OF THE ER				
Redox state of the ER lumen	Assaying the redox state of redox sensitive Fluorescent Proteins	Fluorescence/FACS/Microscopy/ western blot	eroGFP, ER-rxYFGP, Grx-rxYFP,	[37-41, 43, 45-47, 51, 53]
MEASURING CALCIUM DISTRIBUTION				

	GECIs	Florescence/Microscopy	CEPIA family, YC family, D1ER and CatchER	[68-70]
	(TED)	Florescence/Microscopy	GFPCES3, Fluo 5N/Ca+2	[109]
	membrane-targeted GECIs	Florescence/Microscopy	OER-GCaMP6f, Lck-GCaMP6f, LcK-RCaMP2	[73]
	Gaussia Luciferase SERCaMP	Luminescence	SERCaMP	[110]

Table2: Chemical and genetic tools to assess ER stress in mammalian cells

Table3: List of sequences of published primers used to assess ER stress and the unfolded protein response by RT-qPCR and PCR reactions in human and mouse samples.

Pathway		Gene	Human	Mouse (5'- '3)
IRE1□	RIDD	BLOC1S1	5'-CCCAATTTGCCAAGCAGACA-'3 5'-CATCCCCAATTTCCTTGAGTGC-'3 [117]	5'-CAAGGAGCTGCAGGAGAAGA-'3 5'-GCCTGGTTGAAGTTCTCCAC-'3 [11]
		SCARA3	5'- CGCTGCCAGAAGAACCTATC-'3 5'- AACCAGAGAGGCCAACACAG-'3 [118]	5'-TGCATGGATACTGACCCTGA-'3 5'-GCCGTGTTACCAGCTTCTTC-'3 [11]
		PDGFRB	TCCATCCCTCTGTTCTCCTG CTGCCCTCTCCCAGTTATCA [118]	5'-AACCCCCTTACAGCTGTCCT-'3 5'-TAATCCCGTCAGCATCTTCC-'3 [11]
		PMP22	5'-CTGGTCTGTGCGTGATGAGTG-'3 5'-ATGTAGGCGAAACCGTAGGAG-'3 [119]	5'-TGCGATACAGCAGAATGGAG-'3 5'-TTGGTGGCCAATACAAGTCA-'3 [11]
		Col6A1	5'- CCCTCGTGGACAAAGTCAAG-'3 5'- GTTTCGGTCACAGCGGTAGT-'3 [118]	5'-TGCTCAACATGAAGCAGACC-'3 5'-TTGAGGGAGAAAGCTCTGGA-'3 [11]
		GALNT10	5'-ACAGCCAGGTAATGGGTGAG-'3 5'-GAAGATGGGATGGCTTTTCA-'3 [120]	5'-CCTTAGAGATGCTGGGATCG-'3 5'-TGAGGACTCAACTCCCCTTG-'3 [11]
	XBP1s	XBP1spl. (PCR)	5'-GGAGTTAAGACAGCGCTTGGGGA-'3 5'-TGTTCTGGAGGGGTGACAACTGGG-'3 [121]	5'-AGGAAACTGAAAAACAGAGTAGCAGC-'3 5'-TCCTTCTGGGTAGACCTCTGG-'3 [122]
	XBP1s miR-17	XBP1 spl. (qPCR)	5'-TGCTGAGTCCGCAGCAGGTG-'3 5'- GCTGGCAGGCTCTGGGGAAG-'3 [123]	5'-GAGTCCGCAGCAGGTG-'3 5'-GTGTCAGAGTC-CATGGGA-'3 [124]
		MANF	5′-TCACATTCTCACCAGCCACT-'3 5′-CAGGTCGATCTGC TTGTCATAC-'3 [125]	5'-AGGTCCACTGTGCTCAGGTC-'3 5'-CCACCATATCCCTGTGGAAA-'3 [126]
		TXNIP	5'-CTTGCGGAGTGGCTAAAGTG-'3 5'-TTGAAGGATGTTCCCAGAGG-'3 [127]	5'-TCAAGGGCCCCTGGGAACATC-'3 5'-GACACTGGTGCCATTAAGTCAG-'3 [91]
ATF6	ATF6	BIP	5'- TGTTCAACCAATTATCAGCAAACTC-'3 5'- TTCTGCTGTATCCTCTTCACCAGT-'3 [123]	5'-TCAGCATCAAGCAAGGATTG-'3 5'-AAGCCGTGGAGAAGATCTGA-'3 [122]
		PDIA4	5′-AGTGGGGAGGATGTCAATGC-'3 5′-TGGCTGGGATTTGATGACTG-'3 [116]	5′-GGGCTCTTTCAGGGAGATGG-'3 5′-GGGAGACTTTCAGGAACTTGGC-'3 [83]
		HYOU1	5′-GCAGACCTGTTGGCACTGAG-'3 5′-TCACGATCACCGGTGTTTTC-'3 [116]	5'-GTGATAGTGCAGCCGGCAT-'3 5'-AACGGAGCGTAGCCTTTGG-'3 [104]
		SEL1L	5′-ATCTCCAAAAGGCAGCAAGC-'3 5′-TGGGAGAGCCTTCCTCAGTC-'3 [116]	5'-TGGGTTTTCTCTCTCTCCTCTG-'3 5'-CCTTTGTTCCGGTTACTTCTTG-'3 [128]
		EDEM1	5′-TTCCCTCCTGGTGGAATTTG-'3 5′-AGGCCACTCTGCTTTCCAAC-'3 [116]	5'-GGGACCAAGAGGAAAAGTTTG-'3 5'-GAGGTGAGCAGGTCAAATCAA-'3 [128]
		HERPUD1	5′- CGTTGTTATGTACCTGCATC-'3 5′- TCAGGAGGAGGACCATCATTT-'3 [129]	5′-CAGTTGGAGTGTGAGT-'3 5′-CAACAGCAGCTTCCCAGAATA-'3 [129]
		XBP1	5'-TAAGACAGCGCTTGGGGATG-'3 5'-GCACGTAGTCTGAGTCGTGC-'3 [123]	5′-AAGAACACGCTTGGGAATGG-'3 5′-ACTCCCCTTGGCCTCCAC-'3 [124]
PERK	ATF4	CHOP	5'- CAGAACCAGCAGAGGTCACA-'3 5'- AGCTGTGCCACTTTCCTTTC-'3 [123]	5'-CACATCCCAAAGCCCTCGCTCTC-'3 5'-TCATGCTTGGTGCAGGCTGACCAT-'3 [122]
		GADD34	5'- CCTCTACTTCTGCCTTGTCTCCAG-'3 5'-TTTTCCTCCTTCTTCTCGGACG-'3 [118]	5'- CTTTTGGCAACCAGAACCG-'3 5'-CAGAGCCGCAGCTTCTATCT-'3 [130]
		NOXA	5'-TTTCTTCGGTCACTACACAACG-'3 5'-GAGCATTTTCCGAACCTTTAGA--'3 [131]	5'-GACAAAGTGAATTTACGGCAGA-'3 5'-GGTTTCACGTTATCACAGCTCA-'3 [131]
	NRF2	HMOX1	5'-ACTGCGTTCCTGCTCAACATC-3'	5'-GCCGAGAATGCTGAGTTCATG-3'

			5’-GCTCTGGTCCTTGGTGTCATG-‘3 [132]	5’-TGGTACAAGGAAGCCATCACC-3’ [132]
		NQO1	5’-ATGTATGACAAAGGACCCTTCC-‘3 5’-TCCCTTGCAGAGAGTACATGG-‘3 [133]	5’-CGCCTGAGCCCAGATATTGT-3’ 5’-GCACTCTCTCAAACCAGCCT-3’ [132]

Figure Legend

Figure 1: Summary of the activation of the different signaling outputs during ER stress. in green Redox state: eroGFP, rxYFP (1,2); in black ER structure: ThioflavinT (ThT) (3); in red Calcium status: CEPIA (4); Unfolded Protein Response: in orange PERK pathway (5), in violet ATF6 pathway (6); in blue IRE1a pathway (7).

Acknowledgements

This work was funded by grants from Institut National du Cancer (INCa PLBIO), Fondation pour la Recherche Médicale (FRM, équipe labellisée 2018), ANR (ERAAT), MSCA RISE-734749 (INSPIRED) grants to EC. DS was supported by an AIRC fellowship for Abroad.

Author contribution

DS, ADM, LC, EC, AI conceptualized and wrote the manuscript.

Conflicts of interest

EC is a founding member of Cell Stress Discoveries Ltd (https://cellstressdiscoveries.com/)

Supplementary information

Supplementary protocols are listed in the appended PDF file

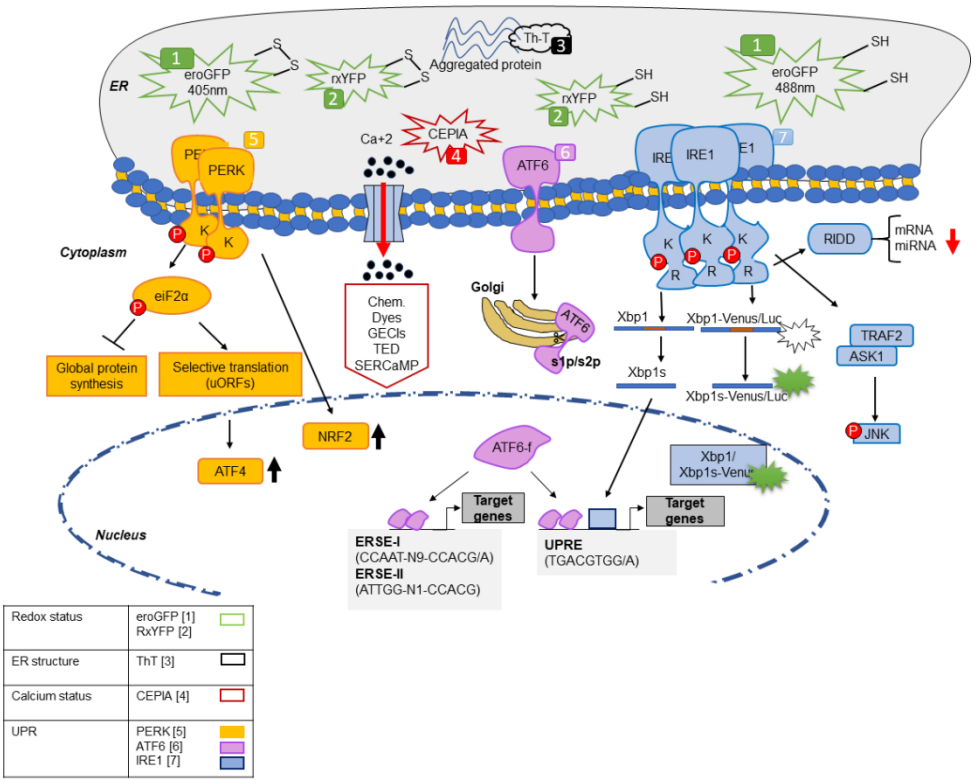

febs_15107_f1.tif